A Potential Solution for MTC: Multi-Carrier Compressed Sensing Multi-User Detection

Fabian Monsees, Matthias Woltering, Carsten Bockelmann, and Armin Dekorsy
Department of Communications Engineering
University of Bremen, Germany
E-mail: {monsees,woltering,bockelmann,dekorsy}@ant.uni-bremen.de

***Abstract*—Compressed Sensing Multi-User Detection is a recently developed physical layer method to decrease signaling in massive Machine communications by using means from the field of Compressed Sensing and sparse signal processing. Within this work we use the advances of recent research and present a non-coherent CS-MUD system concept basing on a combination of multi-carrier modulation and CDMA. This so called Multi-Carrier Compressed Sensing Multi-User Detection (MCSM) concept aims at multiplexing machine-to-machine traffic in narrow band transmissions over the radio resources. Using non-coherent modulation schemes further decreases the needs for pilot symbols and increases robustness with respect to carrier frequency offsets.**

I. Introduction

Machine Type Communication (MTC) is one of the big drivers for future communication systems. In contrast to human driven communications, MTC involves traffic between autonomous entities without human interaction. MTC traffic differs in a variety of parameters from traffic caused by humans. Exemplary, many MTC applications such as sensor networks, smart meters or medical applications are of very low data rate and MTC devices are inactive for most of the time, yielding sporadic traffic [1]. Integrating sporadic and low data rate traffic in today's cellular systems such as 3GPP Long Term Evolution (LTE) is inefficient as medium access via access reservation protocols was designed for high data rates. Here, sporadic MTC traffic easily leads to situations, where the signaling overhead for medium access is greater than the payload, which is clearly ineffective [2], [3].

A novel physical layer approach to reducing signaling overhead for medium access is direct random access. Here nodes directly send their data packets without previous signaling. Thus, the receiver has to detect the activity of the nodes and the data. This approach is known as Compressed Sensing based Multi-User Detection (CS-MUD) [4]–[6] and utilizes algorithms from sparse signal processing and Compressed Sensing to estimate the activity of MTC terminals and the corresponding data. Specifically, CS-MUD exploits the sparsity induced from the sporadic MTC traffic to set up a novel physical layer approach.

This work uses recent advances in CS-MUD and presents a novel multi-carrier narrow band system addressing key aspects such as massive access, flexible spectrum allocation and bandwidth efficiency. This so called Multi-Carrier Compressed Sensing Multi-User Detection (MCSM) system efficiently combines three physical layer technologies to achieve aforementioned goals [7]. To flexibly allocate MTC traffic to radio resources, i.e., in the time-frequency grid, MCSM uses a combination of multi-carrier concepts and Code Division Multiple Access (CDMA). This allows multiplexing MTC traffic inside the coherence bandwidth of the channel. Here we can employ non-coherent modulation and receiver concepts that decrease the need for pilot overhead for channel estimation, while giving some degree of robustness with respect to minor time/frequency offsets. Finally, we use CS-MUD techniques to jointly estimate the activity and the data of the nodes. CS-MUD also allows to efficiently detect MTC traffic, while only using a low number of radio resources. This means systems can be overloaded in the classical sense. In [7] we introduced the general MCSM system concept and evaluated the performance in an uncoded setup. Additionally, we demonstrated MCSM in a hardware setup including a line of sight and a non line of sight setup. The results were presented in [8]. This paper augments previous analysis in the application of channel codes, advanced processing steps and analysis of MCSM under asynchronous transmissions.

We first review the MCSM system model with the underlying sparse MTC traffic model in section II. Here, we also describe the processing at the MTC terminals and the multiplexing of MTC nodes in the frequency domain. Subsequently, in Section III we state the non-coherent detection model that describes a so-called Multiple Measurement Compressed Sensing (MMV-CS) problem [9]. Finally, we prove the feasibility of MCSM in a realistic propagation environment including frequency selectivity and asynchronicity in Section IV.

II. System Concept

The following section presents the general MCSM system concept including the node processing and the time-frequency mapping. While MCSM offers the possibility to multiplex several narrow band MCSM subsystems simultaneously, we restrict ourself without loss of generality to the description of one particular MCSM subsystem with K nodes. Multiplexing of several MCSM subsystems is explained later on. The general system topology is shown in Fig. 1. Here, K nodes transmit frames of L_{Fr} symbols to a central base-station for further processing. Fig. 1 also shows that not all nodes are active all the time but sporadically transmit frames to the base-station. This traffic model is captured by the node specific

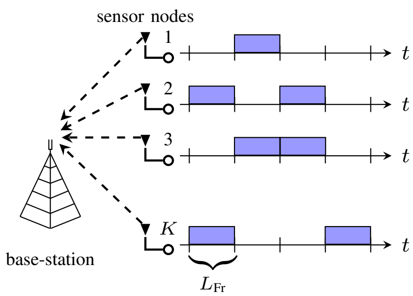

Fig. 1. Machine to machine uplink scenario with K nodes transmitting frames of length L_{Fr} to a central base-station.

activity probability $p_{\text{a}} \ll 1$, which we assume to be the same for all the nodes in the system. With probability p_{a}, a node is active and transmits a data frame to the base-station, while $1 - p_{\text{a}}$ denotes the probability that the node is inactive. Adaptations of the underlying CS-MUD algorithms for other traffic models have been investigated in [10]. Furthermore, we assume a slotted ALOHA scheme, where the time is divided into slots and active nodes transmit for the duration of a slot.

A. MCSM Node Processing

In the following we describe the MCSM transmit signal generation at node k as also depicted in Fig. 2. As nodes can either be active or inactive, our subsequent detection model captures inactivity as modeling inactive nodes as transmitting with zero power. Consequently, the following describes the signal generation at one particular node that is assumed to be active. First, a data stream of L_{a} bits, $\mathbf{a} \in \mathbb{F}_2^{L_{\text{a}}}$ is encoded into

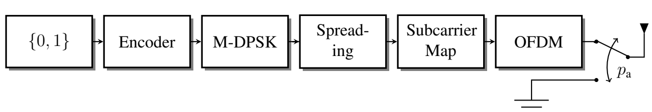

Fig. 2. Block diagram of signal generation at MCSM node.

a stream of code bits $\mathbf{c} \in \mathbb{F}_2^{L_{\text{c}}}$, here $\mathbb{F}_2$ denotes the binary field. Subsequently, the stream of code bits is interleaved and further differentially modulated via a Differential M-Phase Shift Keying (D-MPSK) and the ith modulation symbol reads $b(i) = c(i-1)b(i-1)$ with an arbitrary known starting phase $b(0) = 1$. The next stage spreads the modulation symbols to chips via an unique node specific spreading sequence $\mathbf{s}_k \in \mathbb{C}^{N_{\text{s}}}$. The last step in the MCSM signal generation is to multiplex the chips to physical resources, i.e, to the time-frequency grid. While other concepts are possible, we restrict ourself in this paper to Orthogonal Frequency Division Multiplexing (OFDM) that divides the available bandwidth into N sub-carriers. Here, we multiplex the chips of the spread modulation symbol $\mathbf{s}_k b_{k,i}$ to $\mathcal{P}(i) \subseteq \{0, ..., N-1\}$ sub-carriers of the overall N sub-carriers by using a power normalized partial IDFT matrix $\mathbf{F}_{\mathcal{P}(i)}^H \in \mathbb{C}^{N \times |\mathcal{P}(i)|}$ at the transmitter. Adding a cyclic prefix (CP) as guard interval of length L_{CP} via the CP insertion matrix $\mathbf{T}_{\text{I}} \in \mathbb{F}_2^{N+L_{\text{CP}}N}$ yields the following description of the baseband transmit signal $\mathbf{u}_{k,i}$ in vector notation for node k and symbol i

$$\mathbf{u}_{k,i} = \mathbf{T}_{\text{I}} \mathbf{F}_{\mathcal{P}(i)}^H \mathbf{s}_k b_{k,i} \quad . \tag{1}$$

As shown in (1) the set $\mathcal{P}(i)$ determines the sub-carriers that are allocated for transmission. Without loss of generality, we assume $|\mathcal{P}(i)| = N_{\text{s}} \ \forall i$, i.e., the spreading factor matches the number of sub-carriers allocated. Further, the sub-carrier allocation $\mathcal{P}(i)$ may change according to a predefined pattern yielding a frequency hopping. This procedure enables frequency diversity gains by reallocating the sub-carriers every N_{p} OFDM symbol and can be used if several MCSM systems are multiplexed to a certain bandwidth. Figure 3 illustrates

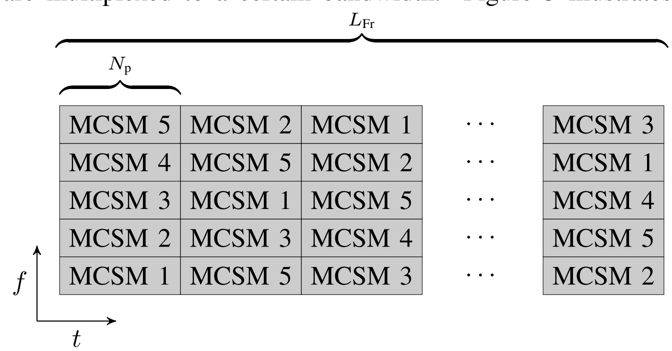

Fig. 3. Illustration of possible scheduling. Each MCSM systems changes its sub-carrier allocation each N_{p} symbols to gain frequency diversity.

this reallocation exemplary in a setup with 5 MCSM systems, where each MCSM system changes its sub-carrier allocation after N_{p} transmit symbols and, thus, gains frequency diversity due to the encoding and interleaving across the time symbols. Assuming that each OFDM symbol carries one modulation symbol $b_{k,i}$ this reallocation leads to a rate loss of $1/N_{\text{p}}$, which is caused by differential modulation where the first transmit symbol carries the starting phase and no information. Complex scheduling algorithms can be avoided, by implementing a static hopping pattern which is repeated each frame.

B. Resource Efficient Sub-Carrier Mapping

Beyond frequency hopping, MCSM implements a resource efficient sub-carrier mapping that is outlined in the following. In each MCSM system, we map the spread modulation symbols $\mathbf{s}_k b_{k,i}$ from overall K nodes to a set of N_{s} sub-carriers. Conventional systems have at least K radio resources for serving K nodes. In MCSM, we aim at serving K nodes with $N_{\text{s}} < K$ radio resources, yielding an overloaded system in the classical sense. This is only possible by using advanced detection schemes that exploit the sparsity in the multi-user signal to still recover the data of the nodes.

The mapping from chips to sub-carriers allows some degree of freedom to trade-off between data rate and robustness. Within this work we assume a simple one-to-one mapping of chips to sub-carriers, i.e, as also shown in Fig. 4 the chip sequence $\mathbf{s}_k b_{k,i}$ is mapped along the frequency direction to a set of N_{s} sub-carriers. Moreover, N_{s} is chosen such that

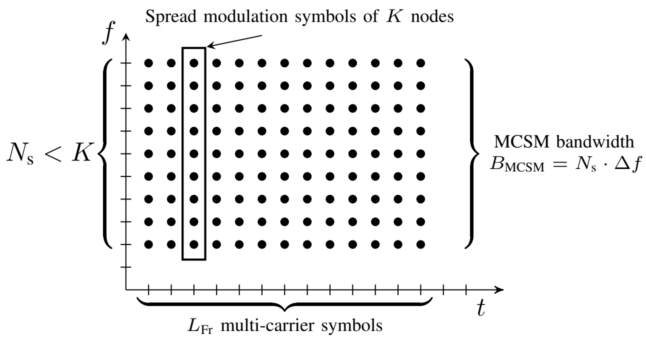

Fig. 4. Illustration of one-to-one mapping of spread sequences over N_s sub-carriers.

the spread sequence lies within the coherence bandwidth of the wireless channel. For the detection described in section III this means that the multi-user interference has to be resolved by a multi-user detector along the frequency axis while the differential demodulation and the encoding works over the time axis. Depending on the coherence time and coherence bandwidth, the multi-user detection suffers from frequency selectivity, e.g., if the coherence bandwidth assumption is violated, while the differential demodulation suffers if the coherence time is too short. Depending on coherence time and coherence bandwidth, chips can also be mapped along the time axis. Moreover, both mappings can be mixed, yielding a joint time-frequency mapping, which allows a flexible link adaptation.

For all possible mappings, the ratio of users to radio resources (sub-carriers in our system) determines the resource efficiency of the system. In section IV we will consider a system, where this ratio is $\beta = K/N_\text{s} = 3$.

III. Detection Model

The following section mathematically formalizes the MCSM system model and states the detection model at the base-station. According to the description above, the received signal at the base-station can be described via the superposition of transmit signals of K nodes. The first processing step at the base-station is to remove the guard interval via the CP removal matrix $\mathbf{T}_\text{R} \in \mathbb{F}_2^{N\times(N+L_\text{CP})}$, subsequently the time domain signal is transformed into frequency domain. Thus, we can describe the ith received symbol in frequency domain in vector notation as

$$\mathbf{y}_i = \sum_{k=1}^{K} \mathbf{F}_{\mathcal{P}(i)}\mathbf{T}_\text{R}\mathbf{H}_k\mathbf{T}_\text{I}\mathbf{F}^H_{\mathcal{P}(i)}\mathbf{s}_k b_{k,i} + \mathbf{n}. \tag{2}$$

Here, $\mathbf{H}_k \in \mathbb{C}^{(N+L_\text{h}-1)\times N}$ denotes the convolution matrix of the underlying wireless channel of node k with length L_h and $\mathbf{n}$ denotes the frequency domain i.i.d. circular symmetric white Gaussian noise vector with zero mean and variance σ_n^2. Note that the circulant matrix $\mathbf{T}_\text{R}\mathbf{H}_k\mathbf{T}_\text{I} = \mathbf{F}^H\mathbf{V}_k\mathbf{F}$ can be expanded via its eigenvalue decomposition, where $\mathbf{F} \in \mathbb{C}_k^{N\times N}$ denotes a N-DFT matrix and the diagonal matrix $\mathbf{V}_k \in \mathbb{C}_k^{N\times N}$ contains the N channel coefficients of node k in frequency domain on its main diagonal. Subsequently, we make use of the assumption that the spreading factor coincides with the coherence bandwidth, justifying the assumption of a single tap channel in frequency domain. Mathematically, we have $\mathbf{F}_{\mathcal{P}(i)}\mathbf{T}_\text{R}\mathbf{H}_k\mathbf{T}_\text{I}\mathbf{F}^H_{\mathcal{P}(i)} \approx h_k(i)\mathbf{I}_{N_\text{s}}$, where $\mathbf{I}_{N_\text{s}}$ denotes the N_s dimensional identity matrix and $h_k(i)$ denotes the single tap channel from user k in frequency domain at transmit symbol i. This connection allows to simplify (2) to

$$\mathbf{y}_i = \sum_{k=1}^{K} h_k(i)\mathbf{s}_k b_{k,i} + \mathbf{n} = \mathbf{S}\tilde{\mathbf{b}}_i + \mathbf{n}, \tag{3}$$

where the columns of $\mathbf{S} \in \mathbb{C}^{N_\text{s}\times K}$ contains the spread symbol $\mathbf{s}_k b_{k,i}$ of the K nodes and $\tilde{\mathbf{b}}_i \in \mathbb{C}^K$ contains the differentially modulated symbols from the K nodes weighted with the individual frequency domain channel, i.e., the kth entry $\tilde{b}_{k,i} = h_k(i)b_{k,i}$ contains the weighted modulation symbol of node k at time instance i. This simple model can easily be extended to capture frame based transmissions of the nodes. In the following we first assume synchronous transmissions, asynchronous transmissions are considered later on. Assuming that all nodes transmit frames of length L_Fr, we obtain

$$\mathbf{Y} = \mathbf{S}\tilde{\mathbf{B}} + \mathbf{N}, \tag{4}$$

where $\mathbf{Y} \in \mathbb{C}^{N_\text{s}\times L_\text{Fr}}$ contains the L_Fr received chips as column vectors. Eq. (4) is the MCSM detection model to detect the activity of all K nodes and the corresponding transmit data at the base-station. Note that (4) is under-determined due to the fact that we use less radio resources than nodes. According to the underlying traffic pattern, the matrix $\tilde{\mathbf{B}}$ is a row-sparse matrix. Recovering $\tilde{\mathbf{B}}$ from $\mathbf{Y}$ is a so-called Multiple Measurement Vector Compressed Sensing (MMV-CS) problem. MMV-CS problems have been widely discussed in literature. For further details the reader is referred to [9] and references therein. In this paper we use the Matrix SIC (M-SIC) algorithm from [11] to solve (4). The M-SIC algorithm basically detects active and inactive nodes by their transmit power and exploits the fact that inactive nodes do not transmit any power. A detailed description and analysis of the M-SIC algorithm can be found in [11].

Robustness to Asynchronicity

At its core, MCSM uses CS-MUD techniques, which themselves have shown robustness against asynchronicity. As shown in [12] the CS-MUD detector can be extended by so called delay hypothesis, which increase the complexity of the detection drastically. In contrast to that, MCSM can inherently cope with asynchronous transmissions without increasing the detection complexity as long as the maximum asynchronicity is restricted to the length of the cyclic prefix in time domain, i.e., the cyclic prefix has to match the length of the channel impulse response and the expected time shift from asynchronous transmissions. Clearly, extending the cyclic prefix to cope with asynchronicity leads to a loss in spectral efficiency.

Subsequently, we assume that the receiver performs an N-point FFT to transform the received signal into frequency domain. In this case, we can measure the time shift in samples $\Delta\tau$ and the correspondence between time and frequency domain yields

$$\mathbf{r}\left[\tau-\Delta\tau\right] \circ\!\!-\!\!\bullet \; \mathbf{y}\left[v\right]\exp\left(\frac{-j2\pi v\Delta\tau}{N}\right), \tag{5}$$

where $\mathbf{r}\left[\tau\right]$ denotes the sampled time domain receive signal prior to an N-point FFT, i.e., $0 \leq v \leq N-1$. As we assume a one-to-one mapping from chips to sub-carriers, the chip sequence is affected by a phase shift. Assuming our MCSM system occupies N_{s} consecutive sub-carriers inside the spectrum, we can write the phase shifts as

$$\mathbf{D} = \left[\mathbf{dg}\left(\mathrm{e}^{\frac{-j2\pi 1}{N}}, \mathrm{e}^{\frac{-j2\pi 2\Delta\tau}{N}}, \ldots, \mathrm{e}^{\frac{-j2\pi N_{\mathrm{s}}\Delta\tau}{N}}\right)\right]^{v_0}. \tag{6}$$

Here, v_0 in the exponent denotes the first sub-carrier that is occupied by the corresponding MCSM system and $\mathbf{dg}\left(\cdot\right)$ sets up the $N_{\mathrm{s}} \times N_{\mathrm{s}}$ dimensional diagonal matrix. Subsequently, we can write the phase shift in our MCSM detection model as

$$\mathbf{Y} = \mathbf{DS\tilde{B}} + \mathbf{DN}. \tag{7}$$

However, $\mathbf{D}$ is unknown to the receiver and, thus, degrades the performance as shown later. As time shifts lead to phase shifts over sub-carriers, possible solutions are 1) to change the chips to sub-carrier multiplexing, i.e., multiplexing in time direction instead of frequency direction, or 2) decrease the spreading sequence lengths with the drawback that fewer nodes can be supported within one MCSM system.

IV. Performance Analysis

In this section we analyze the performance of MCSM in an MTC propagation scenario. More specifically, we demonstrate the performance of one particular MCSM system as several systems can be multiplexed in frequency domain accordingly. The system considered serves $K = 60$ nodes which are spread to chips with sequences of length $N_{\mathrm{s}} = 20$. Subsequently, we map the chips in a one-to-one mapping to $N_{\mathrm{s}} = 20$ sub-carriers. This leads to a system load of $\beta = 3$ nodes per resource. We further assume a delay spread length in meter of the wireless channel of $d_{\max} = 1000$m which yields a coherence bandwidth of $B_c \approx \frac{c_0}{d_{\max}} = 300$kHz and a channel impulse response duration of $\tau_{\mathrm{h}} = 3.33\mu$s. Moreover, we assume an exponentially decaying channel with a path loss exponent of $\epsilon = 2$ with block fading. The remaining simulation parameters are summarized in Table I.

Number of Nodes	$K = 60$
Spreading length	$N_{\mathrm{s}} = 20$
Allocated sub-carriers per MCSM system	$\lvert\mathcal{P}(i)\rvert = 20$
System load	$\beta = 3$
Payload size	$L_{\mathrm{a}} = 300$ Bits
Activity Probability	$p_{\mathrm{a}} = 0.1$
Modulation Type	4-DPSK
Channel Code	(5,7) Convolutional + CRC
Interleaver	Random
Power Control	Perfect
Delay Spread Length	1000 m
Fading Model	Block fading
Number of total sub-carriers	$N = 2048$
CS-MUD detector	M-SIC [11]

TABLE I
SIMULATION PARAMETERS

Fig. 5 plots the Frame Error Rate (FER) for different data rates over the inverse noise variance which is proportional to the Signal-to-Noise-Ratio (SNR). The MCSM system reallocates the sub-carrier set $\mathcal{P}(i)$ each $N_{\mathrm{p}} = 10$ multi-carrier symbols to gain frequency diversity. The plot shows the FER for different data rates by making the time domain symbol shorter, yielding a higher bandwidth occupancy in frequency domain. More specifically, the occupied bandwidth is $B_{\mathrm{MCSM}} = N_{\mathrm{s}}\Delta f = \frac{R_{\mathrm{b}}}{1-R_{\mathrm{b}}L_{\mathrm{CP}}}$, which is $B_{\mathrm{MCSM}} = 40$ kHz for $R_{\mathrm{b}} = 2$ kBit/s and $B_{\mathrm{MCSM}} = 120$ kHz for $R_{\mathrm{b}} = 50$ kBit/s. Note that the noise variance determines the total noise within the bandwidth that the particular MCSM system occupies. This is done to emphasize the effect of frequency selectivity on the MCSM system, without taking the SNR loss due to the higher bandwidth occupation into regard. We clearly see that increased data rates gracefully decrease the FER performance, due to the increased bandwidth and, consequently, increased frequency selectivity of the channel. Additionally, we see that a low data rate MCSM system of $R_{\mathrm{b}} = 2$ kBit/s achieves a frame error rate lower than 10^{-3}, which is reasonable, if we look at one shot transmissions without employing Automatic Repeat Request (ARQ) protocols.

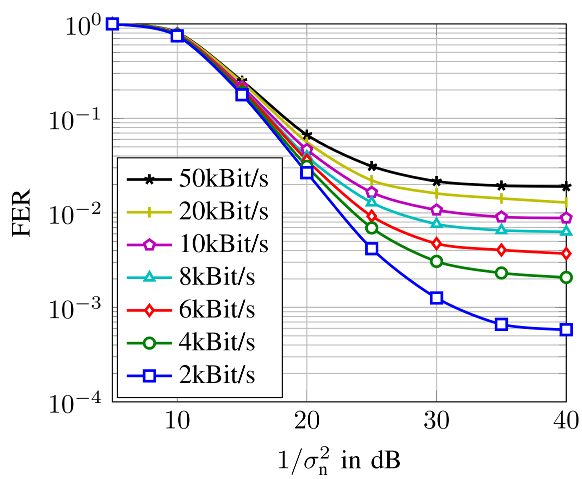

Fig. 5. FER over inverse noise variance for different data rates R_{b}.

Fig. 6 shows the impact of the frequency hopping on the FER performance for a fixed data rate of $R_{\mathrm{b}} = 2$ kBit/s. Decreasing N_{p} leads to a more frequent reallocation of the sub-carriers for the MCSM system and, thus, increased frequency diversity, yielding performance gains. Here, $N_{\mathrm{p}} = \infty$ denotes no sub-carrier reallocation. Note that in the current setting we have a rate-loss of $1/N_{\mathrm{p}}$, i.e., 10% for $N_{\mathrm{p}} = 10$ and 5% for $N_{\mathrm{p}} = 20$, respectively, due to the differential modulation. The results show that one has to trade-off between diversity gains and rate loss due to the differential modulation concept.

The robustness against asynchronicity is shown in Fig. 7, here we plot the asymptotic FER in the noise free region with

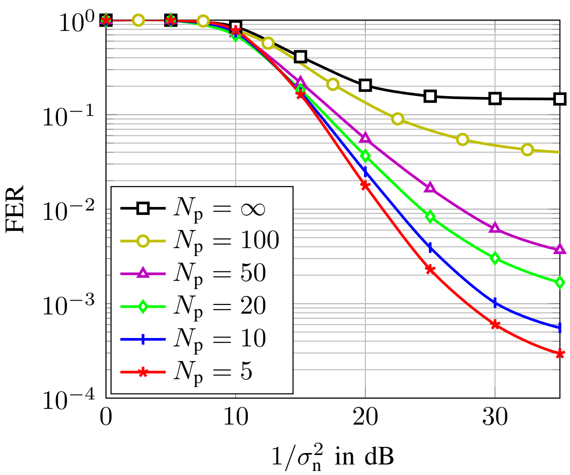

Fig. 6. Performance of MCSM including frequency hopping over the inverse noise variance at a data rate of $R_\mathrm{b} = 2$ kBit/s.

maximum asynchronicity of $\Delta\tau_\mathrm{max}$. Moreover, we assume that the asynchronicity is i.i.d and uniformly between $[0, \Delta\tau_\mathrm{max}]$ for all nodes in the MCSM system. As expected, increased asynchronicity decreases the asymptotic FER. However, the effect of asynchronicity is dependent on the data rate and system with higher data rates suffer more than system with lower data rates. First, the CS-MUD detector has to cope with the unknown frequency selectivity that distorts the spreading sequences due to the violation of the coherence bandwidth, second, we have the unknown phase shift that also distorts the chip sequence according to (7). Combining both effects leads to a decreased performance at higher data rates. However, we see that with $R_\mathrm{b} = 1$ kBit/s, we can support asynchronicity up to 6 μs with FER $< 10^{-2}$.

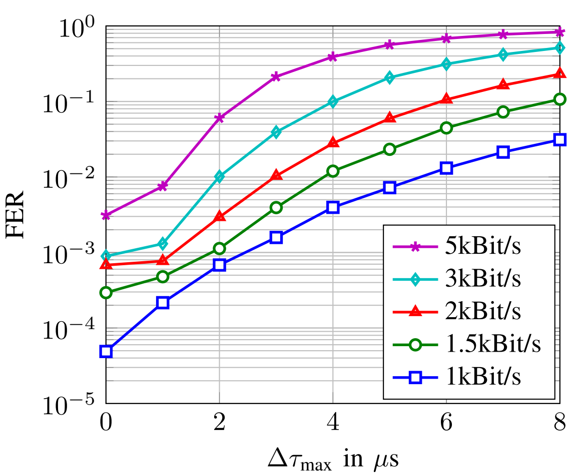

Fig. 7. Asymptotic FER for MCSM with uniform asynchronicity among nodes of up to $\Delta\tau_\mathrm{max}$

V. Conclusion

In this work we have augmented previous advances on Multi-Carrier Compressed Sensing Multi-User Detection (MCSM). While introducing channel coding and advanced processing steps in terms of gaining frequency diversity, we have also shown that MCSM is also robust against asynchronous transmissions. We have shown significant performance gains by reallocating the used frequency band within a transmit frame. This, in turn, comes at the cost of small losses in data rate or payload. In summary MCSM is a candidate technology for direct random access in sporadic massive machine-to-machine communications.

Acknowledgment

This work was funded by the German Research Foundation (DFG) under grants DE 759/3-1 and WU 499/10-1. Parts of this work have been performed in the framework of the Horizon 2020 Project FANTASTIC-5G under Grant ICT-671660, which is partly funded by the European Union.

References

[1] Z. M. Fadlullah, M. M. Fouda, N. Kato, A. Takeuchi, N. Iwasaki, and Y. Nozaki, "Toward Intelligent Machine-to-Machine Communications in Smart Grid," *IEEE Communications Magazine*, vol. 49, no. 4, pp. 60–65, 2011.

[2] Y. Chen and W. Wang, "Machine-to-Machine communication in LTE-A," in *Vehicular Technology Conference Fall (VTC 2010-Fall), 2010 IEEE 72nd, Ottawa, Canada*, Sep. 2010.

[3] R. Ratasuk, N. Mangalvedhe, A. Ghosh, and B. Vejlgaard, "Narrowband LTE-M System for M2M Communication," in *Vehicular Technology Conference (VTC Fall), 2014 IEEE 80th, Vancuver, Canada*, Sep. 2014.

[4] C. Bockelmann, H. F. Schepker, and A. Dekorsy, "Compressive Sensing Based Multi-User Detection for Machine-to-Machine Communication," *Transactions on Emerging Telecommunications Technologies: Special Issue on Machine-to-Machine: An emerging communication paradigm*, vol. 24, no. 4, pp. 389–400, Jun 2013.

[5] H. F. Schepker and A. Dekorsy, "Sparse Multi-User Detection for CDMA Transmission using Greedy Algorithms," in *8th International Symposium on Wireless Communication Systems (ISWCS' 11)*, Aachen, Germany, Nov. 2011, pp. 291 –295.

[6] F. Monsees, C. Bockelmann, D. Wübben, and A. Dekorsy, "Sparsity Aware Multiuser Detection for Machine to Machine Communication," in *Second International Workshop on Machine-to-Machine Communication at IEEE Globecom 2012*, Anaheim, USA, Dec 2012.

[7] F. Monsees, M. Woltering, C. Bockelmann, and A. Dekorsy, "Compressive Sensing Multi-User Detection for Multi-Carrier Systems in Sporadic Machine Type Communication," in *IEEE 81th Vehicular Technology Conference (VTC2015-Spring)*, vol. 81, Glasgow, Great Britain, May 2015.

[8] C. Bockelmann, F. Monsees, M. Woltering, and A. Dekorsy, "Hardware-In-the-Loop Measurements of the Multi-Carrier Compressed Sensing Multi-User Detection (MCSM) System," in *Jahreskolloquium Kommunikation in der Automation (KommA) 2015*, Magdeburg, Germany, Nov 2015. [Online]. Available: arxiv:1511.09278

[9] S. F. Cotter, B. D. Rao, K. Engan, and K. Kreutz-Delgado, "Sparse Solutions to Linear Inverse Problems With Multiple Measurement Vectors," *IEEE Transactions on Signal Processing*, vol. 53, no. 7, pp. 2477–2488, 2005.

[10] Y. Ji, C. Bockelmann, and A. Dekorsy, "Compressed Sensing Based Multi-User Detection with Modified Sphere Detection in Machine-to-Machine Communications," in *10th International ITG Conference on Systems, Communications and Coding (SCC 2015)*, Hamburg, Germany, Feb 2015.

[11] F. Monsees, C. Bockelmann, and A. Dekorsy, "Reliable Activity Detection for Massive Machine to Machine Communication via Multiple Measurement Vector Compressed Sensing," in *IEEE Globecom Workshops (GC Wkshps), Austin, USA*. IEEE, 2014.

[12] H. F. Schepker, C. Bockelmann, and A. Dekorsy, "Coping with CDMA Asynchronicity in Compressive Sensing Multi-User Detection," in *Vehicular Technology Conference (VTC Spring), 2013 IEEE 77th, Dresden, Germany*, Jun 2013.